

강화 단계가 PLA 매트릭스 나노 복합재의 기계적 및 생체 적합성 특성에 미치는 영향

Hatice Evlen[†] and Gülçin Erel^{*†}

Industrial Design Engineering Department, Technology Faculty, Karabuk University

*Industrial Design Engineering Department, Graduate Education Institute, Karabuk University

(2020년 10월 7일 접수, 2021년 1월 21일 수정, 2021년 2월 24일 채택)

Effect of the Reinforcement Phase on the Mechanical and Biocompatibility Properties of PLA Matrix Nano Composites

Hatice Evlen[†] and Gülçin Erel^{*†}

Industrial Design Engineering Department, Technology Faculty, Karabuk University, 78100, Turkey

*Industrial Design Engineering Department, Graduate Education Institute, Karabuk University, 78100, Turkey

Received October 7, 2020; Revised January 21, 2021; Accepted February 24, 2021

Abstract: In this study, it was aimed to obtain nanocomposite structure with poly(lactic acid) (PLA) matrix and to improve the mechanical and morphological properties of the PLA matrix nano-reinforced composites. Titanium dioxide (TiO₂) and hydroxyapatite (HA) nanoparticles were used as reinforcing elements. Solvent casting particle leaching method was used for the production of the composites. Thermal characterization and compression test of the composite samples were carried out. Microstructural properties and the phases formed on the surface of *in vitro* tested samples were examined. As a result of the study, it was observed that nano-reinforced composites with PLA matrix are biocompatible and apatite formation increases gradually every week. Also the highest compressive strength was obtained in PLA/HA samples, while the lowest was obtained in PLA sample. It was concluded that composites prepared within the scope of the study can be used as artificial tissue scaffolds in biomedical and medical applications.

Keywords: poly(lactic acid), hydroxyapatite, titanium dioxide, biocompatibility, nano composite, tissue scaffold.

Introduction

Structural solutions for the tissues in the human body to perform vital activities or to assist in the realization of these activities are increasing day by day. The most utilized material group in these solutions are biological origin materials. Biomaterials should have the ability to interface with biological systems. These materials replace tissues and organs, to help heal, grow and repair body functions. This situation is based on the compatibility of the human body structure with the material used. Such materials can be natural or can be obtained artificially. As with all other materials; biocompatibility, antibacteriality, anti cancerogenity, suitable mechanical strength, long fatigue life, low weight/density ratio, low cost and reus-

ability are among the properties sought in these types of materials. Biodegradable materials consist of natural polymers such as starch, cellulose, and protein. They are preferred because they are degradable in nature, reduce environmental pollution and provide solutions to waste problems. Materials such as biodegradable starch and its derivatives, polybutylene succinate (PBS), polyhydroxy butyrate (PHB), polycaprolactone (PCL) and poly(lactic acid) (PLA) are widely used in polymer applications, packaging, agricultural products and in the medical field.¹

PLA is a semi-crystalline or amorphous, rigid thermoplastic polymer. Other features of PLA produced by using plants rich in starch, such as corn, sugar cane and wheat, are biocompatibility and biodegradability.² PLA compositions are used in surgical sutures used to hold the wound together and provide the necessary support. Also, its use in controlled drug release systems has also become widespread.³ Today, many studies are carried out on composite structures with PLA matrix in order to increase the biocompatibility and mechanical strength of

[†]To whom correspondence should be addressed.
hakgul@karabuk.edu.tr, ORCID 0000-0002-8214-6286
gulcin.ere@gazi.edu.tr, ORCID 0000-0003-1235-7106
©2021 The Polymer Society of Korea. All rights reserved.

PLA material. In order to increase mechanical properties in PLA matrix composites, it has been seen that various secondary phase materials such as carbon nano tube (CNT), graphene, silver (Ag), calcium carbonate (CaCO_3), silicate, titanium dioxide (TiO_2) and hydroxyapatite (HA) ($\text{Ca}_{10}(\text{PO}_4)_6(\text{OH})_2$) are used.^{4,5} When these materials are evaluated for biocompatibility, it is understood that hydroxyapatite (HA), known as bone powder, and titanium dioxide (TiO_2) preferred due to its antibacterial properties are at the forefront.⁶⁻⁹

Since the polymers used in medical fields are generally not osteoconductive, composite structures are formed by supporting with a secondary reinforcement element.⁸ By adding HA to the polymer matrix, osteoconductivity and bone binding potential can be improved.⁹ In addition, HA improves the mechanical properties of PLA by taking the role of reinforcing material.⁶ On the other hand, the formation of acidic products as a result of the degradation of PLA can locally lower the pH and trigger foreign body reactions *in vivo*. This can be resolved by including inorganic filling materials such as HA in PLA. PLA improves the weak degradability of HA.¹⁰ It has been determined that PLA/HA based composites have mechanical properties suitable for bone applications.¹¹ HA, known for its good biocompatibility, is the most popular bioceramic material that can chemically bond with living bone due to its bioactive properties and can be used in orthopedics and dental applications.¹² Wei *et al.* observed that the mechanical properties of the PLA/HA based composites increased dramatically when the nano-sized hydroxyapatite added into the composite instead of micron-size hydroxyapatite. In addition, it was also determined that the increase in the amount of nano-HA in PLA/HA films increased apatite formation on the film.¹³ In a study by Tanodekaew *et al.*, bioactivity (ability to bind to live bone tissue, form apatite on the surface) tests were performed on PLA/HA composite samples with a hollow structure. As a result of the study, it was seen that the addition of HA positively affects the osteoconductivity and bone attachment.¹⁴ Mao *et al.*, on the other hand, prepared PLA/EC/HA (Poly (lactic acid)/ethyl cellulose/hydroxyapatite) composite scaffold samples using the solvent cast particle leaching method. They characterized the functional, structural and mechanical properties of the obtained porous scaffolds. They emphasized that when the PLA reinforced with the EC/HA, the mechanical properties of reinforced composites are better than those of the pure PLA in compression test.¹⁵

TiO_2 is an important compound having high strength among the known oxides of titanium and oxygen. Recently TiO_2

nanoparticles have been proposed as an effective filler to create a biodegradable polymer matrix as it improves cell adhesion on composite surfaces. It has been emphasized in various studies that TiO_2 nanoparticles can be a bioactive material that can provide interfacial binding to tissue.¹⁶

The solvent casting particle leaching technique is based on the production of porous structures by dispersing the solid particles called pore-forming porogen in the matrix material and then removing them from the structure with a suitable solvent. This method is a simple and traditional method used as it allows the creation of pores of the desired size and quantity, and complex equipment is not used. Water-soluble salt or sugar particles are generally preferred as porogen.¹⁷ Selection of solvent material is important in preparing the solution. There are disadvantages such as the inability to completely remove the toxic solvent from the polymer and the degradation of other molecules that joined the polymer. When choosing a solvent material, attention should be paid to the properties such as the boiling and melting point of the solvent, its density, dissolution in water *etc.*¹⁸

The aim of this study is to produce PLA matrix nano-reinforced PLA/HA/ TiO_2 composite samples that are more compatible with the body by using solvent casting particle leaching technique and to examine the produced samples in terms of mechanical and morphological properties.

Experimental

Materials and Methods. Information is available regarding the experimental procedure for the preparation of PLA/HA/ TiO_2 composites by using solvent particle leaching method and also regarding the details of bioactivity test, thermal and morphological analyzes (see Supporting Information).

Results and Discussion

Bioactivity Test. The surfaces of PLA, PLA/HA, PLA/HA/0.5% TiO_2 , PLA/HA/1% TiO_2 , PLA/HA/1.5% TiO_2 samples were examined through scanning electron microscopy (SEM) in order to see the effect of immersing time in simulated body fluid (SBF) in apatite morphology. Accordingly, SEM images of PLA and PLA/HA samples, obtained before immersing in SBF and after immersed on SBF for 4 weeks, are given in Figure 1.

When the SEM images given in Figure 1 are examined, it is seen that HA reinforcement to the PLA matrix material

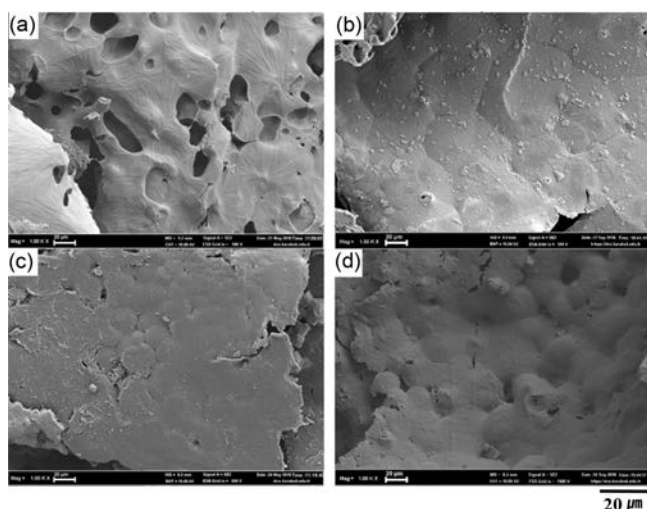


Figure 1. Apatite formation surface SEM images of PLA and PLA/HA samples: (a) PLA not immersed in SBF; (b) PLA immersed for 4 weeks in SBF (c) PLA/HA not immersed in SBF; (d) PLA/HA immersed for 4 weeks in SBF.

increases the formation of apatite on the sample surface. This situation can be understood from the fact that the surface morphologies of PLA/HA samples in Figure 1(c) have smaller porous and rougher than do have PLA samples. After the *in vitro* test, a thicker and wider apatite layer forms on the surface of the PLA/HA samples compared to pure PLA samples. As a result of keeping the PLA samples in SBF for 4 week, it is observed that although apatites occur in a small amount in certain regions, on PLA/HA samples surfaces it is seen that more particulate, rougher surfaces are formed, apatite agglomeration occurs similar to grape grains and apatite formation increases after the same period. EDS analysis after the 4-week *in vitro* test in Figure 6 supports this situation. This situation has also been emphasized in the literature.¹⁹

According to this result, fast apatite formation occurs in PLA/HA. Depending on the increase in calcium content of the surface (at pH=7.4), ions that provide apatite formation are attached to the surface.¹² Since the amount of Ca found in PLA/HA nanocomposite samples is higher than that in pure PLA samples, it can be said that fast and large apatite formation occurs in PLA/HA samples. This situation was emphasized in our previous study.²⁰

The amorphous calcium phosphate phase is formed as a result of apatite calcium phosphate precipitation during the waiting period of the samples in SBF. This amorphous phase first forms a lumpy structure similar to grape bunches and then turns into random big bunches. These clusters are carbonated apatite structures and are also called calcium deficient apa-

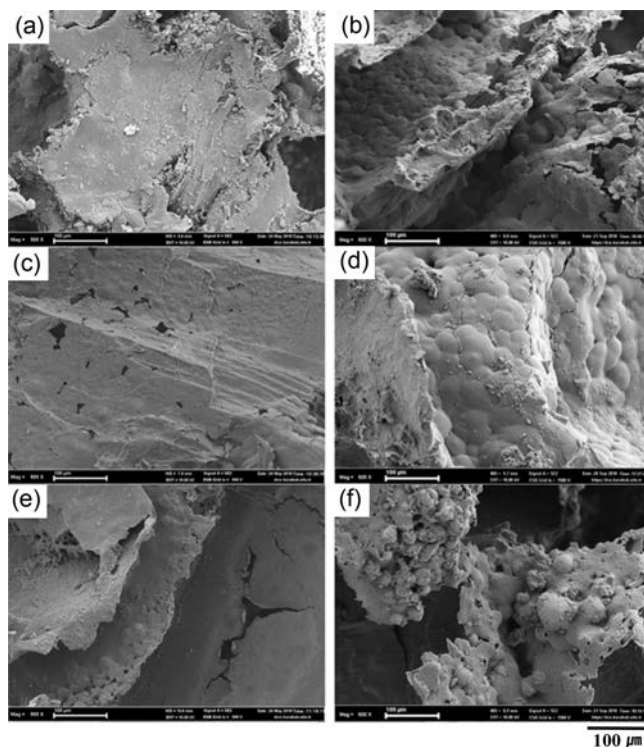


Figure 2. Apatite formation SEM images of TiO₂-reinforced samples: (a) PLA/HA/0.5% TiO₂ samples not immersed in SBF; (b) PLA/HA/0.5% TiO₂ samples immersed in SBF (c) PLA/HA/1% TiO₂ samples not immersed in SBF; (d) PLA/HA/1% TiO₂ samples immersed in SBF; (e) PLA/HA/1.5% TiO₂ samples not immersed in SBF; (f) PLA/HA/1.5% TiO₂ samples immersed in SBF.

tis.¹² In Figure 2, SEM images of the sample surfaces of the PLA/HA/TiO₂ nano composites are given before the *in vitro* and after the 4 weeks *in vitro* test.

When the SEM analysis images from the surfaces of PLA/HA/0.5% TiO₂, PLA/HA/1% TiO₂, PLA/HA/1.5% TiO₂ samples were examined before and after 4 weeks of *in vitro* test, it is clearly seen from Figure 2 that as the immersing time increases in SBF the formation of apatite increases. This situation indicates that the prepared composite materials do not show a negative reaction in body fluid and that the material is a biocompatible composite structure. EDS (Mapping) analysis, given in Figure 3, supports apatite formation as a result of *in vitro* test.

Figure 3(a) and Figure 3(b) shows that the HA layer shows a homogeneous distribution on the entire surface of the PLA and PLA/HA samples, when the TiO₂ is reinforced to composite, the HA layer begins to turn into a grape bunch form, and as the TiO₂ ratio in the composite increases, the clumps of grapes gradually start to grow (Figure 3(c), 3(d), 3(e)). The apatite layer formed on the surface causes an increase in mass

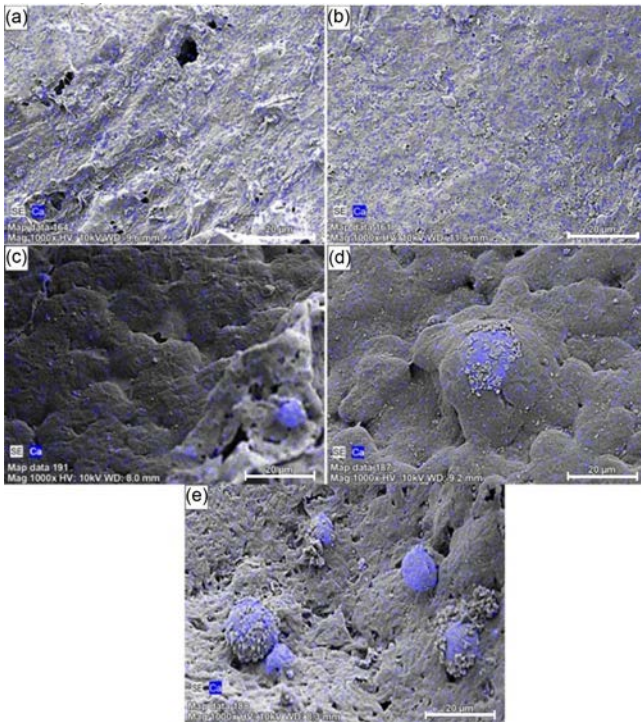


Figure 3. EDS (Mapping) analysis after 4 weeks of *in vitro* test: (a) PLA; (b) PLA/HA; (c) PLA/HA/0.5% TiO₂; (d) PLA/HA/1% TiO₂; (e) PLA/HA/1.5% TiO₂.

in composite samples. This is clearly seen in the weight change graph given in Figure 4.

Comparing the dry weights of composite samples before the *in vitro* test and after 4 weeks of *in vitro* test, it is seen that there is a general increase in the weight of the samples after the bioactivity experiment. This increase indicates the HA formation on the surface of the samples. As a result of the 4 weeks *in vitro* tests, the minimum mass increase was achieved in PLA samples with 94×10^{-4} g, while the maximum mass increase was obtained in PLA/HA samples with 158×10^{-4} g. When 0.5% TiO₂ was reinforced to PLA/HA composite structure, 137×10^{-4} g mass increase occurred, while 1.5% TiO₂ was reinforced, mass increase amount reached 156×10^{-4} grams. This shows that the primary and secondary reinforcement phases added to the PLA material positively affect the formation of apatite on the surface of the sample, the bioactivity and biocompatibility of composites. In addition, the apatite layer increased on the surface of the sample filled the pores in the samples and thus reduced the size of the pores.

The size of the apatite layer formed on the sample surfaces and the change in the size of the pores as a result of the *in vitro* test can be seen in Figure 5. Averages were taken for each parameter by measuring 10 apatite and 5 pore widths from

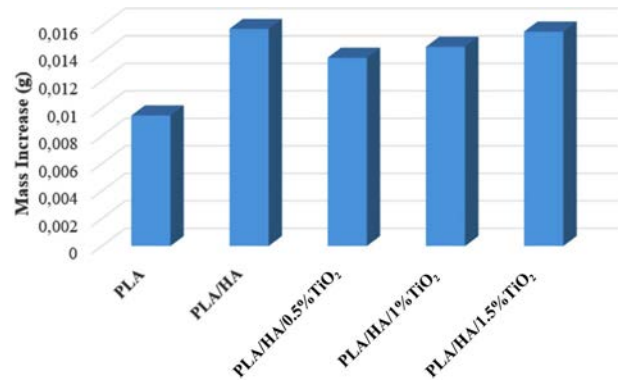


Figure 4. Weight change determined by 4 week Bioactivity test.

each SEM image.

When Figure 5 is examined, it can be seen that the PLA matrix HA and TiO₂ reinforced composite samples' apatite sizes increase with increasing of waiting time in SBF. When the results of the *in vitro* test in the first and fourth weeks were compared, apatite size increase were calculated as 20% in PLA samples, 53% in PLA/HA samples, and 47% in titanium reinforced samples. When evaluated in general, it is seen that as the waiting time in SBF increases, apatite formation increases. While the highest apatite formation was seen in PLA/HA samples, when 0.5% TiO₂ was added to the composite, it was observed that apatite formation decreased and HA formation increased again as the TiO₂ ratio of the composite increased (Figure 5).

As seen in apatite size measurements (Figure 5(a)) and weight changes (Figure 4), the least apatite increase was in PLA samples. When TiO₂ reinforced samples and PLA/HA composites samples compared, it is seen that the apatite formation of PLA/HA samples is higher. Also, according to the mass change graph in Figure 4, the highest mass increase was seen in PLA/HA samples. The mass increase is directly proportional to the apatite formation and inversely proportional to the pore size. In other words, as apatite formation increases in the structure, it is expected that the mass increases and the pore size decreases accordingly. However, since the prepared bio-compatible composite structures are also biodegradable, biodegradation and hence rupture occurred in the samples during *in vitro* tests. Therefore, as a result of the 4-week *in vitro* tests performed, while the greatest reduction in pore size occurred in PLA/HA/0.5%TiO₂ samples, the greatest increase in apatite size and mass was observed in PLA/HA samples (Figure 4 and Figure 5). In addition, as the TiO₂ ratio increases in the composite structure, it is observed that the pore size decreases and

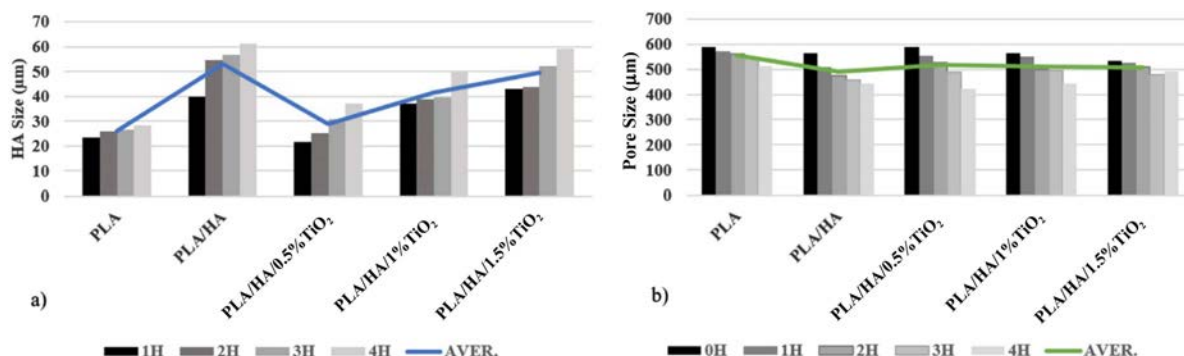


Figure 5. The results of (a) hydroxyapatite; (b) pore size measurement from SEM images.

the mass and apatite size increase. So, it can be said that the increase in the amount of TiO₂ had a positive effect on the formation of apatite. This situation supports the EDS analysis results in Figure 3.

In their study, Aleksandra *et al.* investigated the effect of TiO₂ addition on HA formation. As a result of the study, they emphasized that as the TiO₂ ratio increases, apatite formation on the surface increases as well.²¹ Apatites formed around the pores cause the pore size to shrink.¹⁵ The pore size measurements given in Figure 5 shows that as the waiting time increases in SBF, apatite forms around the pores and these apatites decrease the pore size. Mao *et al.* prepared a composite tissue scaffold containing PLA and HA and examined the bioactivity properties of these structures. In the results of the study, they stated that as the waiting time increases in SBF, apatites formed on the surface cause shrinkage in the pore size.¹⁵ This situation supports the results of this study.

When the pore size shrinkage is calculated as a percentage; the average pore size in non-tested samples decreased by 13% for PLA samples, 22% for PLA/HA samples and 19% for TiO₂ reinforced samples. The greatest pore shrinkage in PLA/HA samples with the highest apatite formation shows that pore sizes are inversely proportional with apatite formation. Also, the pore sizes given in Figure 5 support the results in the weight change plot given in Figure 4. In Figure 6, after 4 weeks bioactivity test, EDS point analysis results are given.

In the SEM images given in Figure 6, it is clearly seen that as the immersing time increases in SBF, more apatite formation occurs. Although there is no hydroxyapatite in the untested PLA samples, as seen in the EDS, 4.72% by weight apatite is formed after immersing in SBF.

In the solvent casting particle leaching method used in the production of test samples, salt (NaCl) particles were used to have a hollow structure of the samples. While the salt and melt

are mixed in the casting process, the salt grains are removed after the drying process. Thus, a hollow structure is obtained by dissolving salt in water. Due to the NaCl residues left on the sample during dissolution, chlorine (Cl) and sodium (Na) peaks are also seen in the EDS results.

While it was determined that the PLA/HA sample kept in SBF for 1 week contains 6.74% Ca by weight, the sample kept for 4 weeks was found to contain 25.09% by weight. From the EDS analysis, it is seen that composite samples with PLA/HA/0.5% TiO₂ composition contain 0.24% Ca by weight after immersing for 1 week in SBF, while samples with the same

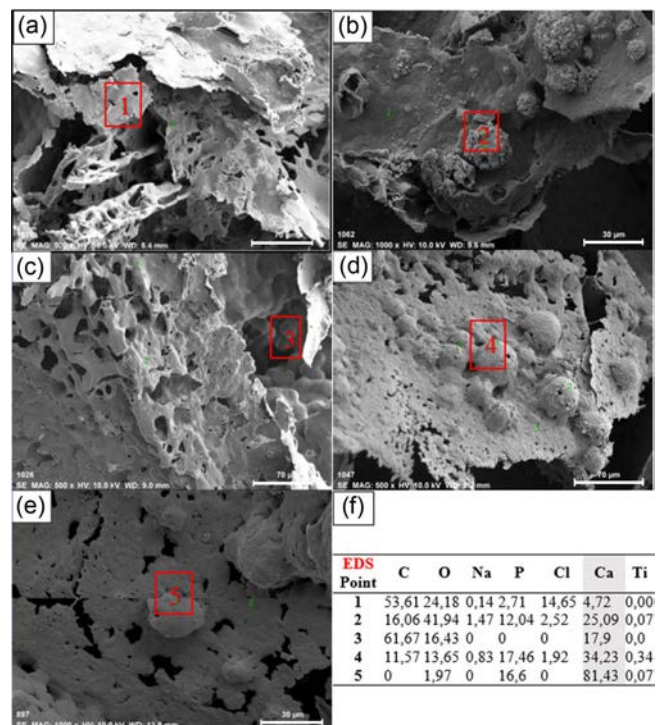


Figure 6. EDS point analysis results after 4 weeks bioactivity test: (a) PLA; (b) PLA/HA; (c) PLA/HA/0.5% TiO₂; (d) PLA/HA/1% TiO₂; (e) PLA/HA/1.5%TiO₂; (f) EDS analysis results for all points.

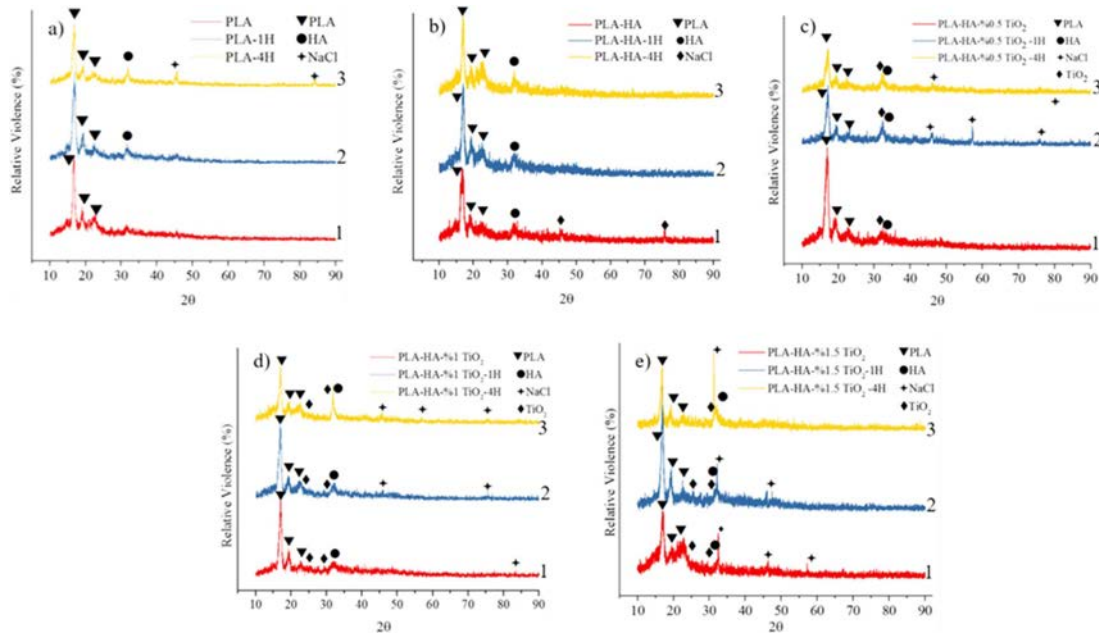


Figure 7. X-ray diffraction (XRD) results of PLA and PLA matrix nano composite samples: (a) PLA; (b) PLA/HA; (c) PLA/HA/0.5% TiO₂; (d) PLA/HA/1% TiO₂; (e) PLA/HA/1.5% TiO₂.

composition contain 17.9% by weight after 4 weeks in SBF. Also, while PLA/HA/1%TiO₂ and PLA/HA/1.5%TiO₂ samples kept in SBF for 1 week contains 0.14% and 4.42% Ca by weight respectively, the same samples kept for 4 weeks were found to contain 34.23% and 81.43% Ca, respectively (Figure 6). This situation supports the increase of apatite formation as the increase of retention time in SBF and increase of TiO₂ ratio of the samples.

X-Ray Diffraction (XRD) Analysis. In Figure 7, the XRD results of PLA matrix composite scaffold samples are given. The number 1 charts in the figure are not kept in SBF, the number 2 charts are kept for 1 week, and the number 3 charts are kept for 4 weeks in SBF.

Figure 7(a) shows the XRD results of the PLA scaffold samples that not immersed in SBF, 1 week immersed and 4 weeks immersed in SBF. When the XRD analysis results are examined, it is seen that apatite formation in the PLA samples that not immersed in SBF is not observed, while it is seen that apatite formation occurs in the samples immersed in SBF for 1 week and 4 weeks. The reason for this is that apatite calcium phosphate precipitation occurs during the waiting period of the samples in SBF followed by the formation of amorphous calcium phosphate phase.¹²

In addition, from the XRD (given in Figure 7) and EDS results (given in Figure 6), it is understood that the increase in the ratio of the TiO₂ reinforcement phase positively affects and

accelerates the apatite formation in the samples, and as the holding time in SBF and the TiO₂ reinforcement phase ratio increase, the apatite formation also increases. In Figure 7(b-e), the XRD results obtained before and after *in vitro* testing of PLA/HA, PLA/HA/0.5% TiO₂, PLA/HA/1% TiO₂, PLA/HA/1.5% TiO₂ samples are given. It is observed from these results that there is little amount of HA phase on the surface of the samples before the *in vitro* test, but there is an increase in the amount of this phase after the *in vitro* test.

Apart from the matrix and reinforcement elements, the XRD results also have NaCl phase. Since the salt used to create pores in the composite sample is not completely dissolved during the dissolution process, thus the NaCl phase was found in XRD analysis. This situation supports the EDS analysis given in Figure 6.

In general, when the peak concentrations of the HA phase obtained are evaluated, it is seen that the HA density increases as the *in vitro* test duration increases.

DTA/TG/DSC Thermal Analysis. Within the scope of the study, after the tissue scaffold with HA and TiO₂ secondary phases with PLA matrix was created, DTA/TG and DSC analyzes were carried out to determine the effect of the secondary phases in these structures on the thermal properties. In Figure 8, TGA analysis results of tissue scaffold samples made of PLA, PLA/HA, PLA/HA/0.5% TiO₂, PLA/HA/1% TiO₂, PLA/HA/1.5% TiO₂ are given.

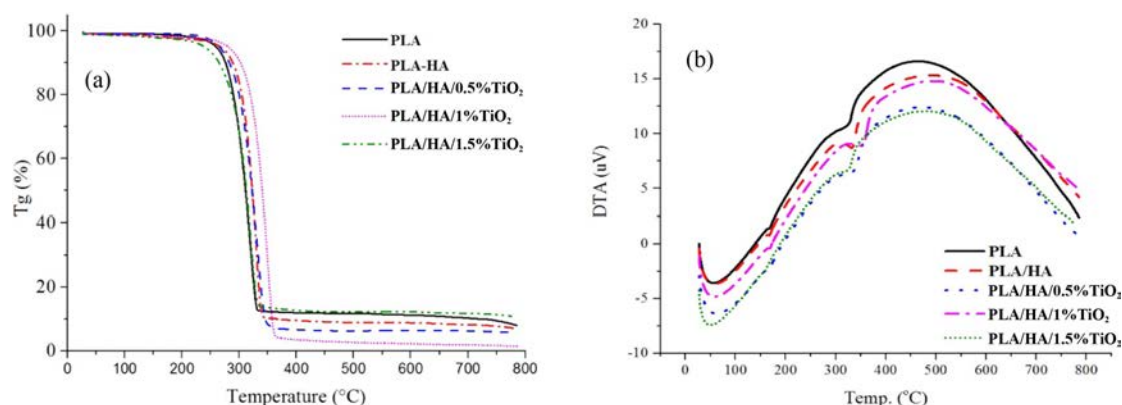


Figure 8. (a) T_g ; (b) DTA results of composite samples.

The decomposition temperatures obtained from DTA/TG plots of PLA and nanocomposite tissue scaffold samples are given in Table 1.

Thermal stability is the resistance of the material to degradation at high temperatures. The increase of decomposition temperatures indicates the increase of thermal stability of the material. When the results of T_g analysis given in Table 1 and Figure 8(a) are examined, it is seen that PLA is degraded between 158–332 °C, when HA and TiO₂ are reinforced to PLA matrix material and composite is formed, the decomposition temperature of the materials increases and reaches up to 159–348 °C range therefore, it is seen that its thermal stability range also increases. The decomposition temperatures of PLA and PLA/HA nanocomposites are lower compared to those of PLA/HA/TiO₂ samples. When the decomposition temperatures of PLA/HA/TiO₂ nanocomposites are compared within themselves, it is seen that the decomposition temperature increases with the increase in the amount of TiO₂. Similarly, in a study by Li *et al.*, it is emphasized that the thermal stability of nanocomposites increases with increasing TiO₂ amount.²²

When the DTA results given in Figure 8(b) are examined, nanocomposite samples showed two different peak points with increasing temperature. The first peak is the material's melting temperature (T_m) and the second is the decomposition temperature (T_d). It is seen from the DTA/TG/DSC curves that the melting temperatures of PLA, PLA/HA, PLA/HA/0.5%TiO₂, PLA/HA/1%TiO₂, PLA/HA/1.5%TiO₂ samples are 158.35, 159.09, 159.52, 159.59, and 161.71 °C, respectively. The decomposition temperatures of the matrix material and nano composite samples were measured in the program called Origin Pro, taking the DTA and T_g curves together. The second peak (T_d) in the DTA curve represents the secondary decom-

Table 1. Degradation Temperatures of PLA Matrix Nanocomposites

Sample name	First decomposition	Second decomposition
PLA	158.35	332
PLA/HA	159.09	340
PLA/HA/0.5% TiO ₂	159.52	351
PLA/HA/1% TiO ₂	159.59	361
PLA/HA/1.5% TiO ₂	161.71	348

(unit: °C)

position point. The decomposition temperature (T_d) is 332, 340, 351, 361, and 348 °C respectively.

In general, it has been determined that reinforcement materials added to composites have a positive effect on thermal stability. While the mass change of composites is recorded as a function of time or temperature in the T_g diagram, in the DTA diagram the rate of mass loss change as a function of time or temperature is recorded. The maximum peak in the DTA diagram shows when the mass change rate and the temperature are greatest.

DSC curves of PLA matrix HA and TiO₂ reinforced composite scaffold samples are given in Figure 9(a-e). T_m , T_g , ΔH , X_c values calculated as the result of the analysis are given in Figure 9(f).

Melting temperatures (T_m), glass transition temperatures (T_g) and melting enthalpies (ΔH_m) of the samples were calculated during the analysis. Using the melting enthalpy value, the degree of crystallinity (% crystallinity) of the polymer in the sample was calculated according to eq. (1).¹⁸

$$\text{Crystallinity (\%)} (X_c) = \frac{\Delta H_m}{93.7} \times 100 \quad (1)$$

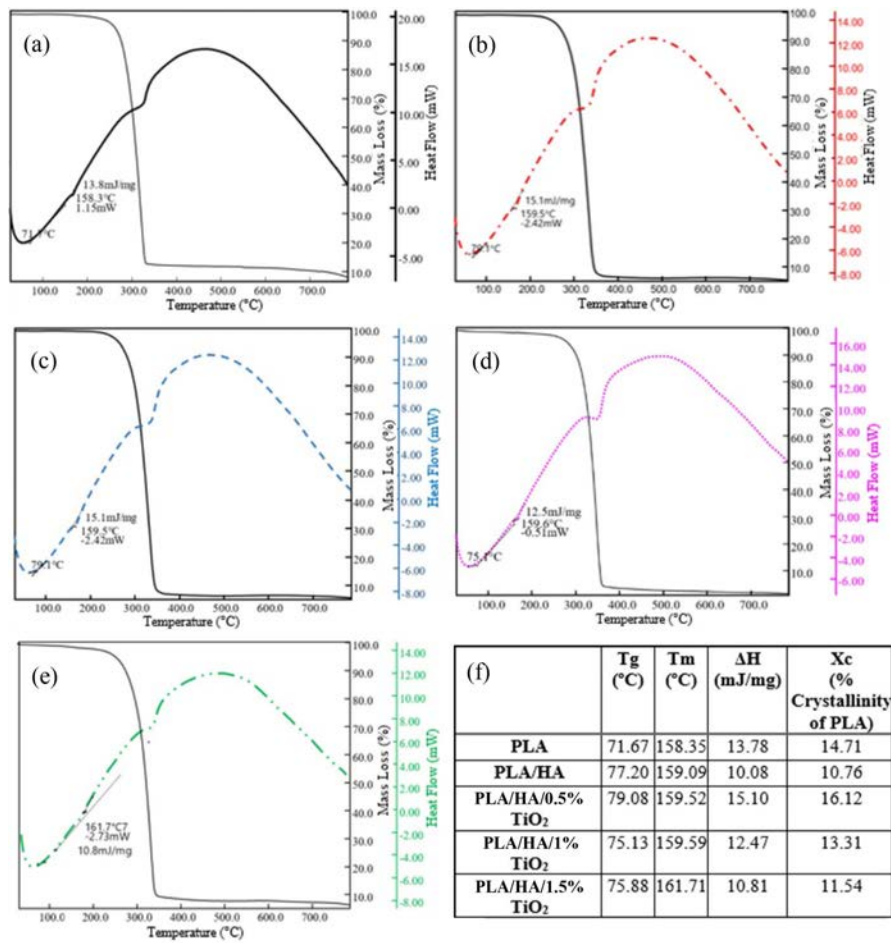


Figure 9. DSC and T_g curves of the samples: (a) PLA; (b) PLA/HA; (c) PLA/HA/0.5% TiO₂; (d) PLA/HA/1% TiO₂; (e) PLA/HA/1.5% TiO₂; (f) Thermal properties of composite samples.

Here ΔH_m indicates the melt enthalpy (J/g), which is the value calculated at the T_m in the DSC curve. The value of 93.7 (J/g) is the theoretical enthalpy value of PLA, which is completely crystalline.¹⁸

Amorphous structure and crystal structure are solid state layouts of polymers. Molecular chains in the amorphous structure are randomly located relative to each other. In the crystal structure, all of the polymer chains are in a certain order. The amorphous structures are hard and brittle below the T_g . As the T_g is exceeded, the structure becomes rubbery. Many commercial polymers such as polyphenylene oxide (PPE), polyvinyl chloride (PVC) are amorphous.²³

While the polymers are solid, they generally have an amorphous and crystalline mixture rather than a hundred percent crystalline structure. PLA is amorphous and crystalline, *i.e.* semi-crystalline. The properties of these plastics depend on the amount of crystalline phase present in the structure.²³ As the

crystallinity increases, the material tends to be more brittle.²⁴ So it is expressed by a factor called X_c (degree of crystallinity). In addition, the melt enthalpy values depend on the crystallinity of the material.²⁵

When Figure 9 is examined, it is seen that the T_m of PLA samples, is 158.35 °C, while the T_m of PLA/HA nanocomposite reaches 159.09 °C. When different amounts of TiO₂ reinforcements are added to the PLA/HA nanocomposites, it is seen that the T_m increases as the rate of reinforcement increases. T_m s of 0.5%, 1% and 1.5% TiO₂ reinforced nanocomposites were obtained as 159.52, 159.59 and 161.71 °C, respectively. This result shows that as the amount of reinforcement in the nano composite structure increases, the melting temperatures of the composite materials also increase. This increase is due to the disintegration (separation) of the chain structures in the polymer by the incorporation of TiO₂ nanoparticles into the structure.¹⁶ This situation is supported by the lit-

erature. Salerno *et al.* studied the PLA/HA composite tissue scaffold and as the result of their study they observed an increase in the T_m values with an increase in the HA ratio.²⁶

Also, it is seen in Figure 9(f) that the T_g of 0.5, 1, and 1.5 TiO₂ reinforced nano composites are 79.08, 75.13, and 75.88 °C, respectively. It is seen that the T_g and the T_m are independent of the TiO₂ reinforcement amount, whereas with increasing TiO₂ amount, the crystallinity of PLA/HA/TiO₂ nano composites decreases. Thus, the energy expended for the melting of the nano composite also decreases.

In his thesis study, Rezwan *et al.* created a biodegradable polymer nano composite structure with PLA matrix using increasing amounts of TiO₂ reinforcement and examined the thermal properties of these structures. As the result of his study, it was stated that T_g and T_m are independent of the amount of TiO₂ added and the crystallinity of composite structures decreases with the increase of TiO₂ reinforcement.¹⁸ These results obtained by Rezwan *et al.* supports this present study.

Compression Test. Information is available regarding the compression test results of the composite samples (see Supporting Information).

Conclusions

When the obtained results are examined, the greatest mass increase and apatite formation were obtained in the PLA/HA samples, while the lowest mass increase and apatite formation were obtained in the PLA sample. When TiO₂ reinforced samples were evaluated among themselves, it was determined that the amount of apatite formed when the amount of TiO₂ reinforcement phase was increased. It was also found that the mass difference increased before and after the bioactivity experiment. Since the apatites formed on the surface cause shrinkage in the pore sizes, the pore size was observed to be inversely proportional to the formation of apatite.

Compression test was carried out to determine the mechanical properties of samples. As a result of the compression test, the highest compression strength was obtained in the PLA/HA samples, while the lowest compression strength was obtained in the PLA samples. It was also observed that as TiO₂ amount increased, the strength of samples increased.

When the compression stress and elasticity results obtained were compared with the literature, the compression stress and elasticities obtained as the result of the experimental study were found to be lower than the values in the literature. The difference between these results is due to the pore sizes in the

samples being larger than the ideal pore size. As a result, the strength causes the cancellous bone structure to be lower than the compression stress (1.9 MPa). The ideal pore diameter for the formation of bone tissue in the literature is 200-350 µm. In the study, the pore size averages in the measurement results were found to be between 490-560 µm. The most important factor affecting the pore size is the size of the salt particles used during production. Another reason that affects the mechanical properties may be the degradation of the PLA polymer by absorbing moisture in contact with oxygen, as a result of which the strength is decreased.

Since the PLA polymer has a semi-crystalline structure, the degree of crystallinity has an effect on mechanical properties. Reinforcements to the polymer matrix disrupt the crystal structure. Therefore, the crystallinity of composite structures created by adding HA and TiO₂ to the PLA matrix is lower than the crystallinity of PLA samples. The degree of crystallinity also affects the hardness and elasticity of the material. While crystallinity and hardness are directly proportional, elasticity is inversely proportional. While HA adds rigidity to the composite structure, TiO₂ adds flexibility. This result was obtained by comparing the modulus of elasticity.

As a result of DTA/TG, DSC thermal analysis, the effect of secondary phase materials reinforced to the matrix on the thermal properties of PLA was analyzed. As the result, it was observed that the secondary phases had a positive effect on the thermal stability of the PLA. With the addition of the secondary phase, decomposition temperatures and melting temperatures increased, and their degree of crystallinity decreased.

As a result of the study carried out, it has been understood that PLA matrix nano composite structures with different reinforcement amounts are suitable for use in health and medical fields in terms of mechanical and thermal properties. Also cell culture studies will be carried out to determine whether the matrix material is biocompatible or not in the next stage of this study.

In addition, it has been concluded that new composite structures can be created by improving the size of salt particles and reinforcement phase percentages used in sample production with the cast particle leaching technique, and thus, superior biological materials can be obtain to use in health and medical fields.

Acknowledgments: The authors thank Scientific Research Project Department of Karabuk University for financial support as part of KBÜBAP-17-YL-441 numbered project.

Supporting Information: Information is available regarding the experimental procedure for the preparation of PLA/HA/TiO₂ composites by using solvent particle leaching method, details of bioactivity test, thermal and morphological analyzes. Information is available regarding the compression test results of the composite samples. The materials are available *via* the internet at <http://journal>.

References

- Dursun, S.; Erkan, N.; Yeşiltaş, M. Doğal Biyopolimer Bazlı (biyobozunur) Nanokompozit Filmler ve su Ürünlerindeki Uygulamaları. *J. of Fish Sci.* **2010**, *4*, 50.
- Henton, D. E.; Gruber, P.; Lunt, J.; Randall, J. Poly(lactic acid) Technology. In *Natural Fibers, Biopolymers, And Biocomposites*; Amar, K. M.; Manusri, M.; Lawrence, T. D., Eds.; CRC Press: Boca Raton, USA, 2005; pp 527-577.
- Nehal, S.; Mohamed, A.; Mohamed, G.; Sahar, E. Synthesis and Design of Norfloxacin Drug Delivery System Based on PLA/TiO₂ Nanocomposites: Antibacterial and Antitumor Activities. *Mater. Sci. and Eng. C* **2020**, *108*, 1-11.
- Almeida, J. F. M.; Silva, A. L. N.; Escócio, V. A.; Fonseca Thom, A. H. M.; Sousa, A. M. F.; Nascimento, C. R.; Bertolino, L. C. Rheological, Mechanical and Morphological Behavior of Poly(lactide)/nano-sized Calcium Carbonate Composites. *Polym. Bull.* **2016**, *73*, 3531-3545.
- Costa, R. G.; Brichi, G. S.; Ribeiro, C.; Mattoso, L. H. Nanocomposite Fibers of Poly(lactic acid)/titanium Dioxide Prepared by Solution Blow Spinning. *Polym. Bull.* **2016**, *73*, 2973-2985.
- Kothapalli, C. R.; Shaw, M. T.; Wei, M. Biodegradable HA-PLA 3-D Porous Scaffolds: Effect of Nano-sized Filler Content on Scaffold Properties. *Acta Biomater.* **2005**, *1*, 653-662.
- Watazu, A.; Kamiya, A.; Zhu, J.; Nonami, T.; Sonoda, T.; Shi, W.; Naganuma, K. Mechanical Properties of Hydroxyapatite-granule-implanted Titanium Alloy. *Key Eng. Mater.* **2003**, *240*, 931-934.
- Kretlow, J. D.; Young, S.; Klouda, L.; Wong, M.; Mikos, A. G. Injectable Biomaterials for Regenerating Complex Craniofacial Tissues. *Adv. Mater.* **2009**, *21*, 3368-3393.
- Nazhat, S. N.; Kellomaki, M.; Törmälä, P.; Tanner, K. E.; Bonfield, W.; Dynamic Mechanical Characterization of Biodegradable Composites of Hydroxyapatite and Poly(lactides). *J. Bio. Mater. Res.* **2001**, *58*, 335-343.
- Senatov, F. S.; Niaza, K. V.; Zadorozhnyy, M. Y.; Maksimkin, A. V.; Kaloshkin, S. D.; Estrin, Y. Z. Mechanical Properties and Shape Memory Effect of 3D-printed PLA-based Porous Scaffolds. *J. Mech. Behav. Biomed. Mater.* **2016**, *57*, 139-148.
- Talal, A.; McKay, I. J.; Tanner, K. E.; Hughes, F. J. Effects of Hydroxyapatite and PDGF Concentrations on Osteoblast Growth in a Nanohydroxyapatite-poly(lactic acid) Composite for Guided Tissue Regeneration. *J. Mater. Sci. Mater. Med.* **2013**, *24*, 2211-2221.
- Demirkol, N. Bioactivity Properties and Characterization of Commercial Synthetic Hydroxyapatite-5 wt% Niobium (V) Oxide-5 wt% Magnesium Oxide Composite. *Acta Phys. Polonica A.* **2017**, *132*, 786-788.
- Wei, G.; Ma, P. X. Structure and Properties of Nanohydroxyapatite/polymer Composite Scaffolds for Bone Tissue Engineering. *Biomater.* **2004**, *25*, 4749-4757.
- Tanodekaew, S.; Channasanon, S.; Kaewkong, P.; Uppanan, P. PLA-HA Scaffolds: Preparation and Bioactivity. *Proced. Eng.* **2013**, *59*, 144-149.
- Mao, D.; Li, Q.; Bai, N.; Dong, H.; Li, D. Porous Stable Poly(lactic acid)/ethyl Cellulose/hydroxyapatite Composite Scaffolds Prepared by a Combined Method for Bone Regeneration. *Carbohydr. Polym.* **2018**, *180*, 104-111.
- Lu, X.; Lv, X.; Sun, Z.; Zheng, Y. Nanocomposites of Poly(l-lactide) and Surface-grafted TiO₂ Nanoparticles: Synthesis and Characterization. *Eur. Polym. J.* **2008**, *44*, 2476-2481.
- Khulbe, K. C.; Matsuura, T.; Feng, C. Processing and Applications. In *Handbook of Polymers for Pharmaceutical Technologies*; Thakur, V. K., Thakur, M. K., Eds.; Scrivener Publishing: Beverly, USA, 2015; p 43.
- Rezwan, K.; Chen, Q. Z.; Blaker, J. J.; Boccaccini, A. R. Biodegradable and Bioactive Porous Polymer/inorganic Compositescaffolds for Bone Tissue Engineering. *Biomater.* **2006**, *27*, 3413-3431.
- Wu, D.; Spanou, A.; Diez-Escudero, A.; Persson, C. 3D-printed PLA/HA Composite Structures as Synthetic Trabecular Bone: A Feasibility Study using Fused Deposition Modeling. *J. Mech. Behav. Biomed. Mater.* **2020**, 103608.
- Evlen, H.; Erel, G. Polimer Matrisli Nano Takviyeli Biyokompozitlerin Biyoaktivite ve Mikroyapı Uygulamaları. *Biomaten 2018 Abstract Booklet*; Ankara, Turkey; 2018; p 89.
- Buzarovska, A.; Gualandi, C.; Parrilli, A.; Scandola, M. Effect of TiO₂ nanoparticle Loading on Poly(L-lactic acid) Porous Scaffolds Fabricated by TIPS. *Composites Part B* **2015**, *81*, 189-195.
- Li, Y.; Chen, C.; Li, J.; Sun, X. S. Synthesis and Characterization of Bionanocomposites of Poly(lactic acid) and TiO₂ Nanowires by *in situ* Polymerization. *Polymer* **2011**, 2367-2375.
- Kodal, M.; Sirin, H.; Ozkoc, G. Effects of Reactive and Nonreactive POSS Types on The Mechanical, Thermal and Morphological Properties of Plasticized Poly (lactic acid). *Polym. Eng. Sci.* **2014**, *54*, 264-275.
- Callister, W. D.; Rethwisch, D. G. Fundamentals of Material Science and Engineering (An Introduction), 8th ed.; Wiley: New York, USA, 2009.
- Kawakami, K. Pharmaceutical Applications of Thermal Analysis. In *Handbook of Thermal Analysis and Calorimetry*; Vyazovkin, S., Koga, N., Schick, C., Eds.; Elsevier: Amsterdam, Netherland, 2018, pp 613-641.
- Salerno, A.; Fernández-Gutiérrez, M.; San Román, J.; Domingo, C. R. Macroporous and Nanometre Scale Fibrous PLA and PLA-HA Composite Scaffolds Fabricated by a Bio Safe Strategy. *Royal Soc. of Chem.* **2014**, *4*, 61491-61502.

Publisher's Note The Polymer Society of Korea remains neutral with regard to jurisdictional claims in published articles and institutional affiliations.